



# Effect of phenolic resin thickness on frequency-dependent dynamic mechanical properties of Nomex honeycomb cores

Yong Zhou<sup>a</sup>, Qinglin Wang<sup>a</sup>, Yunli Guo<sup>a</sup>, Yongzheng Xu<sup>a</sup>, Xiaosu Yi<sup>b</sup>, Yuxi Jia<sup>a,\*</sup>

<sup>a</sup> Key Laboratory for Liquid-solid Structural Evolution & Processing of Materials (Ministry of Education), Shandong University, Jinan, 250061, China

<sup>b</sup> National Key Laboratory of Advanced Composites, AVIC Composites Center, Beijing, 100095, China

## ARTICLE INFO

### Keywords:

Experimental/numerical method  
Damping properties  
Honeycomb  
Mechanical properties

## ABSTRACT

Using the mixed experimental/numerical method, the frequency-dependent transverse shear moduli (TSM) and damping values of the commercially available Nomex honeycomb cores were investigated. Four kinds of honeycomb cores with different phenolic resin thicknesses were used to explore the effect of the phenolic resin thickness on these dynamic mechanical properties. Results reveal that both the TSM and damping values have positive logarithmic relationships with the frequency, and the sensitivity of these dynamic mechanical properties to frequency is higher for the honeycomb core with thicker phenolic resin. Among all the transverse shear directions, TSM and damping values in the LT direction are the highest at medium and high frequencies. Compared with the damping values, the effect of phenolic resin thickness on TSM is more obvious. Therefore, it is a more efficient way to enhance the TSM than to improve the damping values by controlling the thickness of phenolic resin.

## 1. Introduction

Due to the competitive comprehensive properties like low equivalent density, excellent out-of-plane specific stiffness and low dielectric properties, Nomex honeycomb materials are widely used in weight-sensitive fields, such as the aerospace [1] and rail traffic. The Nomex honeycomb is usually manufactured by the stretching expansion process, during which the shape of aramid paper is fixed by the cured phenolic resin, and the viscoelastic phenolic resin is always frequency-dependent. Therefore, the effect of the phenolic resin thickness on the frequency-dependent dynamic mechanical properties is studied. In recent years, not only the safety but also the comfort is receiving more and more attention among the aforementioned service environments.

The safety is mostly guaranteed by good mechanical properties of the honeycomb sandwich structure. Generally speaking, the in-plane properties are mainly provided by the thin and high-stiffness skins while the out-of-plane properties are mainly contributed by the thick and relatively soft core [2,3]. Besides, considering that the out-of-plane (transverse) shear moduli (TSM) of the core play an important role in the determination of modal parameters [4] and wave characteristics [5], the focused mechanical properties of the honeycomb core are the TSM in this study. In addition to the experimental measurements, there are several ways to obtain the TSM such as the analytical method [6], numerical method like finite element method (FEM) [7,8],

experimental/analytical method [9] and experimental/numerical method [3,10,11]. The experimental/numerical method can effectively take the frequency dependence of mechanical parameters into account, which is adopted here. The main process of this method is taking sensitivity analysis of interested parameters firstly, and then obtaining the final parameters when the deviation between the calculated and experimental modal parameters keeps stable at a relatively small value.

The vibration and noise reduction is a vital factor to improve the comfort, which is closely linked to the intrinsic damping properties [5,12]. Although the honeycomb materials have been used for decades, limited works [5,13] have been done to characterize the damping properties of honeycomb core while more studies [14–16] focused on the damping properties of the integrated honeycomb sandwich structure. Adams and Maheri [13] tested the damping values of aluminum and Nomex honeycomb cores by shear testing technique, which are about 0.13% and 1.65%, respectively. Then, these damping parameters were further used to calculate the damping values of honeycomb sandwich beams [17] and panels [2]. Based on the Ross-Ungar-Kerwin model, James Sargianis and Jonghwan Suhr [5] derived the damping values of 2.5%–5.7% for Nomex and 4.2%–8.2% for Kevlar honeycomb cores from the corresponding modal loss factors of honeycomb beams. However, these damping values were not further validated. Though it is important to understand the relationship between the structure (thickness of phenolic resin) and their dynamic mechanical properties,

\* Corresponding author.

E-mail address: [jia\\_yuxi@sdu.edu.cn](mailto:jia_yuxi@sdu.edu.cn) (Y. Jia).

<https://doi.org/10.1016/j.compositesb.2018.08.126>

Received 21 June 2018; Received in revised form 5 August 2018; Accepted 27 August 2018

Available online 29 August 2018

1359-8368/ © 2018 Elsevier Ltd. All rights reserved.

to the authors' knowledge, there is still no published work investigated this relationship and analyzed the sensitivities of these properties to the frequency.

Here, the focus of this paper is not only to obtain and validate the TSM and damping values of the Nomex honeycombs, but also to analyze how the phenolic resin thickness and the frequency affect these parameters and the antagonism between the mechanical properties (TSM) and damping properties. Since the honeycomb core is non-self-supporting material, plenty of sandwich beams with 1060 aluminum as the skins were used to obtain these values in the LT direction and WT direction, whose physical significance is intuitive and clear. Furthermore, several 45°-direction aluminum/honeycomb sandwich beams (the angle between the length direction of the beam and L-direction is 45°) were fabricated to validate the above obtained parameters. Considering the frequency dependence of TSM and damping parameters, the honeycomb sandwich panels with carbon fiber reinforced polymer (CFRP) as skins were studied to further evaluate the effects of the phenolic resin thickness on the damping properties of symmetrical CFRP/honeycomb panel at last.

## 2. Experiments

### 2.1. Materials and fabrication

Four kinds of T722 Nomex honeycomb cores (Shanghai Pengji Co., Ltd.) were investigated in this work; they are NH-1-1.83-48, NH-1-1.83-64, NH-1-1.83-80 and NH-1-1.83-128 with identical cell side length of 1.83 mm and different nominal volume densities of 48 kg/m<sup>3</sup>, 64 kg/m<sup>3</sup>, 80 kg/m<sup>3</sup> and 128 kg/m<sup>3</sup>. Since these honeycomb cores have the same Nomex paper and cell side length, therefore, different volume densities are equivalent to different phenolic resin thicknesses. The material coordinate system of honeycomb core is illustrated in Fig. 1(a) and the basic engineering parameters of aluminum and CFRP skins are listed in Table 1.

The aluminum sandwich beams, unidirectional CFRP laminates and CFRP sandwich panels were fabricated by the hot press process. Thereinto, the aluminum skins and honeycomb cores were bonded by the epoxy adhesive film (Shanghai Gongwo, GW-2095) at 120 °C for 2 h under a nominal pressure of 0.15 MPa. The unidirectional CFRP laminates were fabricated by sixteen-layer unidirectional preregs (Dezhou Furun, TR50S15 L/YPH-308) at 75 °C for 0.5 h and 120 °C for 1.5 h under the pressure of 0.6 MPa. As for the symmetrical CFRP sandwich panels, eight-layer unidirectional preregs were used as skins in the sequence of [45/-45/45/-45/honeycomb core/-45/45/-45/45], and cured with the same pressure as aluminum sandwich beams and the same temperature scheme as unidirectional CFRP laminates.

In order to obtain the damping values of skins or honeycomb cores in a certain frequency range, three groups of specimens with different lengths were prepared for each corresponding type of beams. The

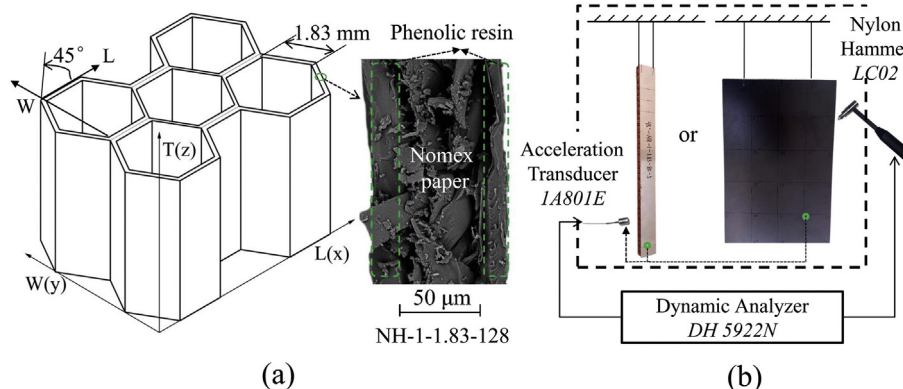


Fig. 1. Material coordinate and corresponding modal testing equipment: (a) Honeycomb coordinate; (b) experimental equipment.

Table 1  
Properties of aluminum and unidirectional CFRP skins.

| Material | $E_{11}$ (GPa) | $E_{22}, E_{33}$ (GPa) | $G_{12}, G_{13}$ (GPa) | $G_{23}$ (GPa) | $\nu_{12}, \nu_{13}$ | $\nu_{23}$ | $\rho$ (kg/m <sup>3</sup> ) |
|----------|----------------|------------------------|------------------------|----------------|----------------------|------------|-----------------------------|
| Aluminum | 70             | 70                     | 25.88                  | 25.88          | 0.33                 | 0.33       | 2705                        |
| CFRP     | 120            | 8                      | 4.18                   | 4              | 0.3                  | 0.35       | 1535                        |

Table 2  
Dimensions of the beams.

| Beams                   | Orientations     | Length (mm) | Width (mm) | Thickness (mm)                  |
|-------------------------|------------------|-------------|------------|---------------------------------|
| CFRP beams              | 0°/45°/90°       | 270/240/210 | 20.0       | 2.1 ± 0.05                      |
| Aluminum beams          | N/A              | 350/310/270 | 32.5       | 6.0 ± 0.05                      |
| Aluminum sandwich beams | L/W <sup>c</sup> | 350/310/270 | 32.5       | 0.945 (skin) × 2 + 12.75 (core) |
|                         | 45°              | 350 or 250  | 32.5       |                                 |
| CFRP sandwich panels    | N/A              | 300 (L)     | 200 (W)    | 0.56 (skin) × 2 + 12.75 (core)  |

<sup>c</sup> Represents that the L-direction or W-direction of the core is parallel to the length direction of beam, and the corresponding beam is denoted by L-direction or W-direction beam in the next sections, respectively.

dimensions of the beams are listed in Table 2. The numbers of parallel specimens were three and five for each type of the aforementioned skin beams and sandwich beams, respectively, and all of the specimens were left at 50 °C for 10 h prior to testing.

### 2.2. Testing process

Fig. 1(b) shows the testing equipment (Donghua Testing Co., Ltd.) sketch, where the force excitation signals are given by the nylon hammer (LC02) and the acceleration response signals are collected by the acceleration transducer (IA801E, weight 1 g). Then, the above signals are digitalized and processed by a dynamic signal analyzer (DH5299 N). Finally, the frequency response functions are obtained by the ratio of response signals and excitation signals after the fast Fourier transform.

Clamping boundary conditions always introduce additional damping, especially for the first modal loss factor [18]. Therefore, all of the specimens are suspended by the thin nylon wires in order to be as close as possible to the free-free boundary conditions. In fact, the excitation and response positions also have a certain influence on the final testing results. In this paper, the excitation position (1/6 of beam length from the top) and the response position (1/15 of beam length from the bottom) were unified for all beams. In the case of the sandwich panels,

**Table 3**  
Deviations between experimental and analytical natural frequencies.

| Mode | Experimental (Hz) | Analytical (Hz) | Deviations (%) |
|------|-------------------|-----------------|----------------|
| 1    | 324.68            | 326.48          | -0.550         |
| 2    | 896.27            | 899.95          | -0.409         |
| 3    | 1757.66           | 1764.26         | -0.374         |
| 4    | 2899.97           | 2916.40         | -0.564         |
| 5    | 4317.55           | 4356.60         | -0.897         |

thirty excitation points were evenly arranged on the specimens, and the response point was put at the lower right corner as shown in Fig. 1(b). According to the coherence function, ten times effective excitations were carried on each excitation point, and the average values were used to calculate the modal parameters including the mode shapes, natural frequencies and modal loss factors. More specifically, the half power bandwidth method [19] was used to obtain the modal loss factors, since the damping values of the investigated honeycomb cores are much smaller than 0.1 [20].

In order to validate the reliability of the equipment, three 1060 aluminum beams were tested firstly with the dimension of 270 × 32.5 × 6 (unit: mm). For the beam at free-free boundary conditions, its analytical bending modal frequencies can be calculated by Eq. (1) [21] with the parameters in Table 1, where  $E$  is elastic modulus;  $I$  is the sectional moment of inertia;  $m$  is the mass per unit length;  $L$  is the length; when the number of mode,  $r \geq 1$ ,  $\lambda_r = (2r + 1) \times \pi/2$ . As shown in Table 3, the deviations between the experimental and analytical natural frequencies are small (less than 0.9%) and the equipment is used in the next sections.

$$f_r = \frac{\lambda_r^2}{2\pi L^2} \left( \frac{EI}{m} \right) \quad (1)$$

After the modal test, the quasi-static three-point bending test is performed on the above L- and W-direction sandwich beams to obtain the TSM of the honeycomb cores [22], using an electronic universal testing machine (SANS CMT4204). The lengths of specimens are unified to 200 mm with a span of 150 mm. A constant cross head velocity of 1 mm/min is adopted to produce failure within 3–6 min [23].

### 3. Theoretical model and finite element analysis

#### 3.1. Theoretical model

The TSM of the honeycomb core are usually at least two orders of magnitude higher than its in-plane moduli [3]. Besides, the strain in the T-direction during bending deformation is usually small. Therefore, the strain energy during deformation in the core is solely contributed by the transverse shear strain energy [2]. Assuming that the specimen damping values are independent of the stresses, the modal loss factor of the honeycomb sandwich structure can be obtained by Eq. (2) based on the modal superposition method.

$$\eta_{sw}^r = \frac{\Delta U_{skin}^r + \Delta U_{hc}^r}{U_{skin}^r + U_{hc}^r} = \frac{\eta_{skin} U_{skin}^r}{U_t} + \frac{\eta_{WT} U_{WT}^r}{U_t} + \frac{\eta_{LT} U_{LT}^r}{U_t} \quad (2)$$

where  $\Delta U$  and  $U$  are the dissipated energy and strain energy, respectively.  $r$  and  $hc$  represents the  $r$ th mode and honeycomb, respectively.  $U_t$  is the total modal strain energy;  $\eta_{skin}$  and  $U_{skin}$  are the damping coefficient and strain energy of the skins, respectively.  $\eta_{LT}$  and  $\eta_{WT}$  are the damping coefficients in the planes (L, T) and (W, T), respectively.  $U_{LT}$  and  $U_{WT}$  are the strain energy associated with the corresponding principle stresses, respectively.

For the orthotropic CFRP skin, its modal loss factor can be obtained by Eq. (3) [24] based on the first shear deformation theory (FSDT).

$$\eta^r = \frac{\eta_{11} U_{11}^r + \eta_{22} U_{22}^r + \eta_{66} U_{66}^r + \eta_{44} U_{44}^r + \eta_{55} U_{55}^r}{U_{11}^r + U_{22}^r + U_{66}^r + U_{44}^r + U_{55}^r} \quad (3)$$

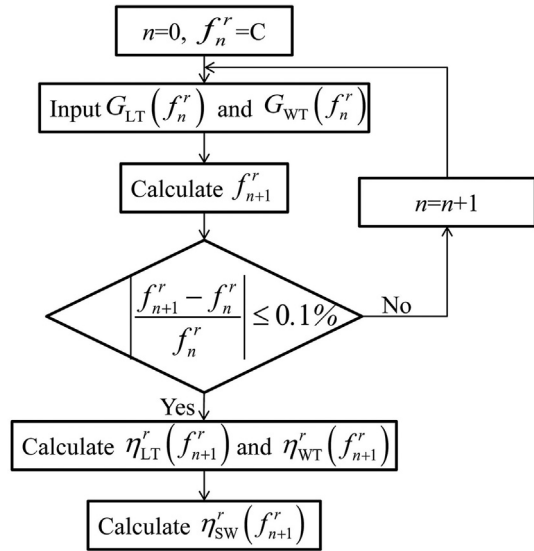


Fig. 2. Calculation process of modal loss factor.

where  $\eta_{11}$  and  $\eta_{22}$  are the damping coefficients of 0° and 90° unidirectional laminates, respectively;  $\eta_{44}$ ,  $\eta_{55}$  and  $\eta_{66}$  are shear damping coefficients.  $\eta_{55}$  is equal to  $\eta_{66}$ .  $\eta_{44}$  has only little effect on the modal behavior of thin skins, which is assigned the same value as  $\eta_{66}$ . So,  $\eta_{66}$  can be obtained by Eq. (3) with an intermediate orientation beam like a 45° unidirectional beam.  $U_{11}$ ,  $U_{22}$ ,  $U_{66}$ ,  $U_{44}$ , and  $U_{55}$  are the strain energy associated with the corresponding principle stresses, respectively.

#### 3.2. Finite element analysis

The modal strain energies mentioned in section 3.1 are calculated by ANSYS 14.5 with element shell181. Since the strain energy associated with the corresponding principle stresses cannot be obtained by ANSYS 14.5 directly, an APDL program was developed to calculate these strain energies. After obtaining the TSM and damping parameters, considering the frequency dependency of these parameters, the modal loss factor calculation process of honeycomb sandwich structures is shown in Fig. 2, where C can be assigned any constant within our interested frequency range of 500–5000 Hz.

### 4. Results and discussion

#### 4.1. Damping parameters of skins

The damping values of 1060 aluminum within 500–4500 Hz are awfully small (0.025–0.14%) as shown in Fig. 3(a), where the loss factors obtained from too sharp unsmooth peaks at the low frequencies are omitted. A fluctuate increasing process takes place below 3000 Hz, and the rising rate becomes faster subsequently. In order to simplify the calculation process, a constant damping value of 0.04% for the 1060 aluminum is used in the remaining sections, and the deviations caused by this constant damping value in the damping parameters acquisition of honeycomb cores will be discussed in Section 4.2.2.

Note that the length of the error bars is twice as much as the corresponding sample standard error ( $S_{n-1}$ ) in Figs. 3, 7 and 8 and  $S_{n-1} \times U_{ij}$  ( $ij = LT, WT$ ) in Fig. 6.

Fig. 3(b) reports the damping values of the CFRP skins as a function of the frequency in 0°, 45° and 90° fiber orientations. Then, the basic damping coefficients of  $\eta_{11}$ ,  $\eta_{22}$ , and  $\eta_{66}$  are obtained by Eq. (3).

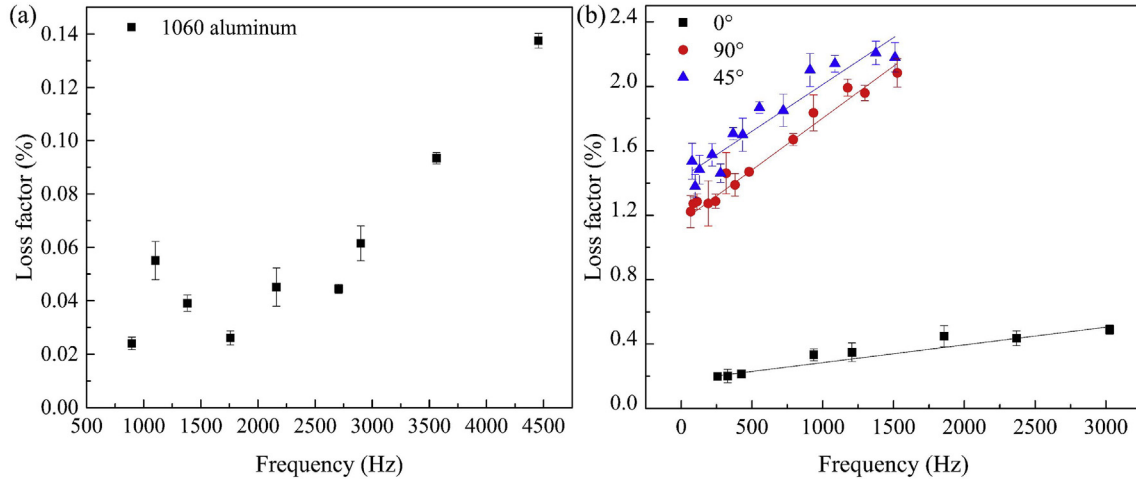


Fig. 3. Damping parameters of skins: (a) Aluminum skins; (b) CFRP skins.

4.2. Effect of phenolic resin thickness on TSM and damping values of honeycomb cores

4.2.1. Effect of phenolic resin thickness (volume density) on TSM

Since the dimensions of the specimens and boundary conditions have been determined, the natural frequencies of the sandwich structure mainly depend on the transverse shear moduli (TSM) of the core and mechanical parameters of the skins. For an L-direction aluminum/honeycomb sandwich beam, the  $G_{WT}$  of the core, as well as the adhesive film have only a marginal effect on its modal behavior based on the sensitivity analysis and modal calculation. Besides, the deviations in Table 3 are almost independent of the frequency, which means that the mechanical parameters of aluminum are scarcely affected by the frequency within 4500 Hz. Therefore, the only unknown  $G_{LT}$  of the honeycomb core under different frequencies can be obtained by fitting the calculated and experimental frequencies. Similarly, the  $G_{WT}$  under different frequencies is obtained from the W-direction sandwich beams.

The TSM of the honeycomb cores show strong positive logarithmic relationships with the frequency in Fig. 4, and these values within 500–5000 Hz are higher than the corresponding results obtained from the quasi-static test as shown in Table 4. As expected, the TSM increase with the increasing phenolic resin thickness. In addition, the slopes of TSM to frequency also increase with the phenolic resin thickness, which means that the TSM of the honeycomb core with high wall thickness (high volume density) have high sensitivity to the frequency.

The Nomex paper usually has a relatively high density, and the phenolic resin is hard to penetrate into the interior of the paper as shown in Fig. 1(a). Assuming that the Nomex paper is homogeneous and isotropic, and the phenolic resin is distributed evenly on its both

Table 4

TSM of honeycomb cores derived from quasi-static test.

| Honeycomb material |           | $G_{LT}$ (MPa) | $G_{WT}$ (MPa) |
|--------------------|-----------|----------------|----------------|
| NH-1-1.83-48       | Mean      | 42.11          | 31.24          |
|                    | $S_{n-1}$ | 1.03           | 1.64           |
|                    | C.V.      | 2.45%          | 5.24%          |
| NH-1-1.83-64       | Mean      | 45.81          | 37.02          |
|                    | $S_{n-1}$ | 2.13           | 2.34           |
|                    | C.V.      | 4.65%          | 6.33%          |
| NH-1-1.83-80       | Mean      | 54.95          | 38.51          |
|                    | $S_{n-1}$ | 2.35           | 4.82           |
|                    | C.V.      | 4.27%          | 12.50%         |
| NH-1-1.83-128      | Mean      | 86.45          | 61.91          |
|                    | $S_{n-1}$ | 8.02           | 4.09           |
|                    | C.V.      | 9.28%          | 6.61%          |

sides. Then, the TSM of the hexagonal honeycomb can be calculated by Eqs. (4) and (5) [6]. Besides, the one-side phenolic resin thickness can be easily obtained under the second assumption by Eq. (6).

$$G_{LT} = \frac{5\sqrt{3}}{9l} (G_{Nomex} t_{Nomex} + 2G_{phenolic} t_{phenolic}) \tag{4}$$

$$G_{WT} = \frac{\sqrt{3}}{3l} (G_{Nomex} t_{Nomex} + 2G_{phenolic} t_{phenolic}) \tag{5}$$

$$t_{phenolic} = \frac{3\sqrt{3}l\rho_c - 8t_{Nomex}\rho_{Nomex}}{12\rho_{phenolic}}, \quad \rho_c \geq \frac{8\sqrt{3}t_{Nomex}\rho_{Nomex}}{9l} \tag{6}$$

where  $l$  is the cell side length;  $G$  is the shear modulus;  $\rho$  is density;  $t$  denotes the thickness and  $\rho_c$  denotes volume density of the honeycomb

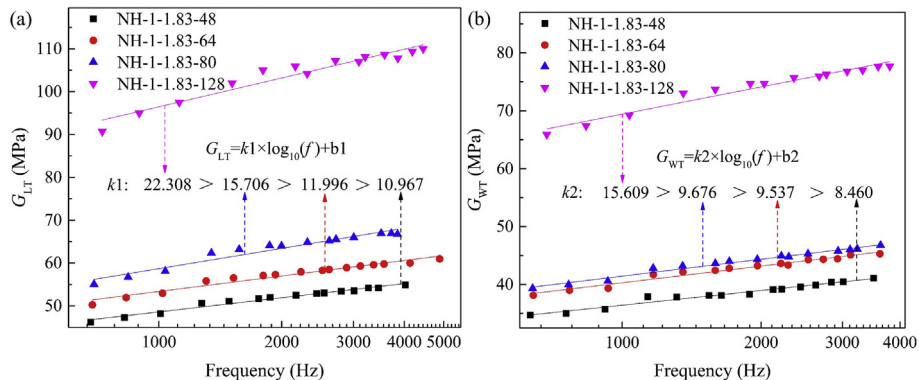


Fig. 4. TSM of honeycomb cores as a function of frequency: (a)  $G_{LT}$ ; (b)  $G_{WT}$ .

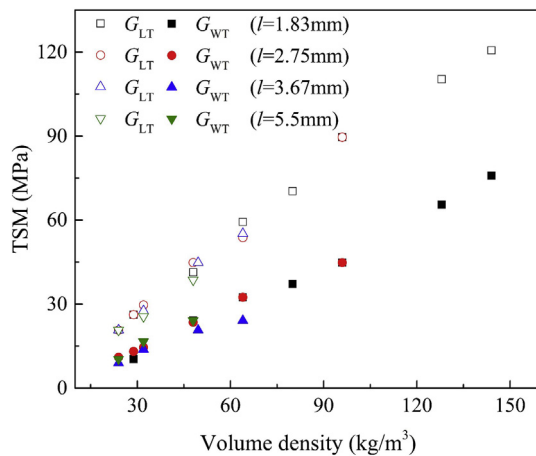


Fig. 5. TSM as a function of volume density for honeycomb cores with different sizes.

core.

Substituting Eq. (6) into Eqs. (4) and (5), respectively, the relationship between TSM and volume density is obtained, and the slopes are  $5G_{\text{phenolic}}/(6\rho_{\text{phenolic}})$  and  $G_{\text{phenolic}}/(2\rho_{\text{phenolic}})$  for  $G_{\text{LT}}$  ( $\rho_c$ ) and  $G_{\text{WT}}$  ( $\rho_c$ ), respectively. It is interesting that the slopes only depend on the type of phenolic resin under aforementioned assumptions, which means no matter what the cell side length of the core is, the rising rate of TSM of hexagonal honeycomb core with volume density are all the same once the type of phenolic resin is determined. For the honeycomb cores with different cell side lengths, their TSM as a function of the volume density from book [25] are plotted in Fig. 5, which shows a relatively good consistency with the theoretical prediction.

#### 4.2.2. Effect of phenolic resin thickness on damping values

After obtaining the TSM of the honeycomb cores, the modal strain energy in Eq. (2) can be calculated, where the  $U_{\text{WT}}$  can be neglected compared with the  $U_{\text{LT}}$  for an L-direction aluminum/honeycomb sandwich beam. Then, the second item on the right side of Eq. (2) becomes zero, and the damping coefficients of  $\eta_{\text{LT}}$  are obtained from the damping values of the sandwich beam. The damping coefficients of  $\eta_{\text{WT}}$  are obtained from W-direction beams in the same way.

From Eq. (2), it is obvious that the higher the strain energy ratio of the aluminum skin is, the greater the deviation caused by the damping value deviation of the aluminum skin will be. Because the strain energy ratios of the skins increase with the increasing TSM of the cores, so the maximum deviation takes place in the damping parameters acquisition of NH-1-1.83-128. As shown in Fig. 3(a), the lowest and highest damping values of the 1060 aluminum are 0.025% and 0.14% at a relatively low frequency and high frequency, respectively. When the damping values of aluminum are assigned 0.04% and 0.025%, respectively, the damping values deviation of NH-1-1.83-128 at about 600 Hz is  $-1.865\%$ ; when the damping values are 0.04% and 0.14%, respectively, the deviation at about 4000 Hz is 0.488%. Therefore, the constant damping value of 0.04% for the 1060 aluminum is used to simplify the calculation process. The damping value of high-strength aluminum alloy was adopted as 0.016% in Ref. [2], and the literature [26] used 0.22–0.32% as the damping value of aluminum in the frequency range of 50–1000 Hz.

The damping values of the four kinds of honeycomb cores are 1.65–2.8% within 500–4000 Hz as shown in Fig. 6. At relatively low frequencies, the damping values of  $\eta_{\text{WT}}$  are slightly higher than  $\eta_{\text{LT}}$ . The situation is opposite at the relatively high frequencies, where the damping values of  $\eta_{\text{LT}}$  are about 7% higher than  $\eta_{\text{WT}}$ . In contrast with the TSM, the damping values of honeycomb cores decrease with the increasing phenolic resin thickness. It should be noted that the damping differences among NH-1-1.83-48, NH-1-1.83-64 and NH-1-1.83-128 are

relatively small. Especially the damping values of NH-1-1.83-80 and NH-1-1.83-64 are roughly equivalent, and this phenomenon corresponds to the differences between their TSM and phenolic resin thickness. As shown in Fig. 4, the TSM differences between NH-1-1.83-64 and NH-1-1.83-80 are also relatively small, especially for the  $G_{\text{WT}}$ . According to the results in Figs. 4 and 6, the NH-1-1.83-80 with relatively low TSM and relatively high damping values shows a certain antagonism between the mechanical properties (TSM) and damping properties of the honeycomb core. Since the type of Nomex paper and phenolic resin are all the same for these four kinds of honeycomb cores, the inconsistent properties of NH-1-1.83-80 is mainly caused by the manufacturing process.

The energy dissipation in the honeycomb core is mostly contributed by the interfacial friction between Nomex paper and phenolic resin, the microfiber friction and intermolecular friction of Nomex paper, as well as the intermolecular friction of phenolic resin. Theoretically, it is hard to form the chemical bond between the phenolic resin and polyisophthaloyl metaphenylene diamine fiber during the manufacturing process of Nomex honeycomb, and a large number of tiny voids exist in the interface region, which means the dry friction within interface is mainly a purely physical process. Therefore, both of the material effect like intermolecular friction of phenolic resin and the structural effect like dry friction within interfacial phase exist in the damping mechanism of the honeycomb material.

The damping value of phenolic resin, tested by DMA in literature [27], is about 1.7% at a low frequency. Therefore, it is highly possible that the dissipated energy per unit strain energy of phenolic resin is relatively lower than that of the other two components, which leads to the tendency of increasing damping value with the decreasing phenolic resin thickness.

As shown in Figs. 4 and 6, the increasing rate of TSM and the decreasing rate of damping values with the increasing phenolic resin thickness (volume density) are different. For example, when the density increases by two times from NH-1-1.83-64 to NH-1-1.83-128, the  $G_{\text{LT}}$  increases by 80.9% at 1000 Hz while the damping values of  $\eta_{\text{LT}}$  decreases by 13.0%. From this perspective, it is a relatively efficient way to enhance its mechanical properties by increasing the thickness of phenolic resin.

#### 4.2.3. Preliminary verification of TSM and damping values of honeycomb cores

Adopting the parameters obtained in above two sections, the first five bending modal frequencies and loss factors of 45°-direction (Fig. 1(a)) aluminum sandwich beams are calculated based on the calculation process in Fig. 2. Then, the calculated results are compared with the experimental results as shown in Fig. 7. The honeycomb core dimensions used in (a), (b) and (d) are  $350 \times 32.5 \times 12.75$ , and in (c) is  $250 \times 32.5 \times 12.75$  (unit: mm). Overall, the deviations between calculated and experimental natural frequencies are basically less than 1% (the maximum deviation is 2.5% for the fourth natural frequency in Fig. 7(c)), and the deviations of modal loss factors are basically less than 2% (the maximum deviation is 7.2% for the first modal loss factor in Fig. 7(c)), which validates the obtained TSM and damping parameters preliminarily.

#### 4.3. Effect of phenolic resin thickness on damping properties of CFRP sandwich panels

Taking NH-1-1.83-64 and NH-1-1.83-128 as examples, the first four modal parameters of symmetrical CFRP honeycomb sandwich panels are calculated considering the frequency dependence of TSM and damping parameters. The calculated and experimental results are illustrated in Fig. 8, where the calculated mode shapes agree well with the experimental results.

For natural frequencies, the calculated values are always larger than the experimental results, which is mainly caused by the one-step

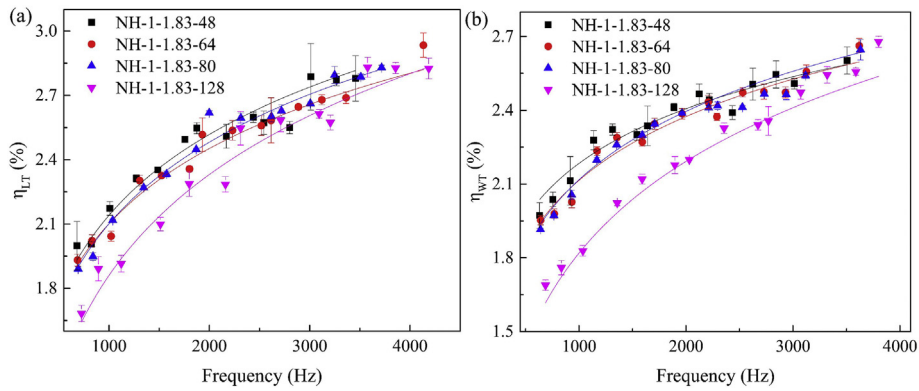


Fig. 6. Damping values of different honeycomb cores as a function of frequency: (a)  $\eta_{LT}$ ; (b)  $\eta_{WT}$ .

forming process. The good surface roughness is hard to be guaranteed during this process, especially for the panels with relatively thin skins. Besides, the forming pressure is smaller than the CFRP laminates. Consequently, the mechanical properties of CFRP skins are lower than the theoretical values, and the natural frequencies decline. The average deviations of the first four natural frequencies between the experiment and calculation are  $-8.75\%$  (maximum:  $-11.01\%$ ) and  $-5.31\%$  (maximum:  $-8.05\%$ ) for these two sandwich panels, respectively.

As for the modal loss factors, the results obtained by FEM and experiment show relatively good consistency. Considering that the air damping has little effect on the beams with little dimensions, but cannot be neglected for the panels with big dimensions [28], the experimental damping values of sandwich panels should be higher than the calculated values in theory. However, the loss factors obtained by experiment are slightly smaller than the calculated values at the low-order vibration modes, which is mainly caused by the mechanical parameters deviation of the CFRP skins as mentioned above. The overestimated mechanical values lead to higher natural frequencies and

lower strain energy ratio of skins. On the one hand, overestimated natural frequencies further lead to overestimated damping parameters of CFRP skins since the damping values of skins increase with the increasing frequency. On the other hand, overestimated strain energy ratio of honeycomb core leads to higher damping values of the sandwich structure since the damping values of honeycomb cores are slightly higher than the CFRP skins at the relatively low frequencies. The strain energy ratio of skins decreases with the increasing vibration mode, which leads to relatively little impact of mechanical parameters deviation of the CFRP skins on the high order modal loss factors.

The calculated average modal loss factors of the same four modes are 1.74%, 1.69%, 1.64% and 1.46% for the investigated four kinds of symmetrical CFRP/honeycomb sandwich panels, respectively. Relatively thinner phenolic resin leads to relatively lower TSM and higher damping values of the honeycomb core, and the lower TSM further leads to higher strain energy ratio of the honeycomb core, which result in relatively higher damping values of the sandwich structures.

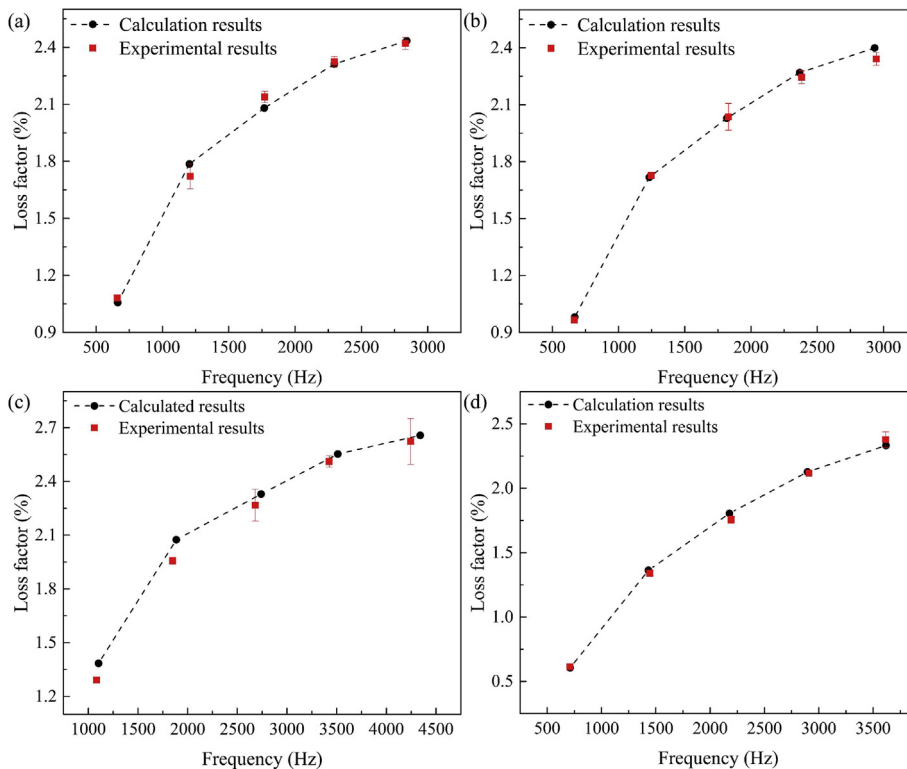


Fig. 7. First five bending modal frequencies and loss factors obtained by FEM and experiment: (a) aluminum/NH-1-1.83-48; (b) aluminum/NH-1-1.83-64; (c) aluminum/NH-1-1.83-80; (d) aluminum/NH-1-1.83-128.

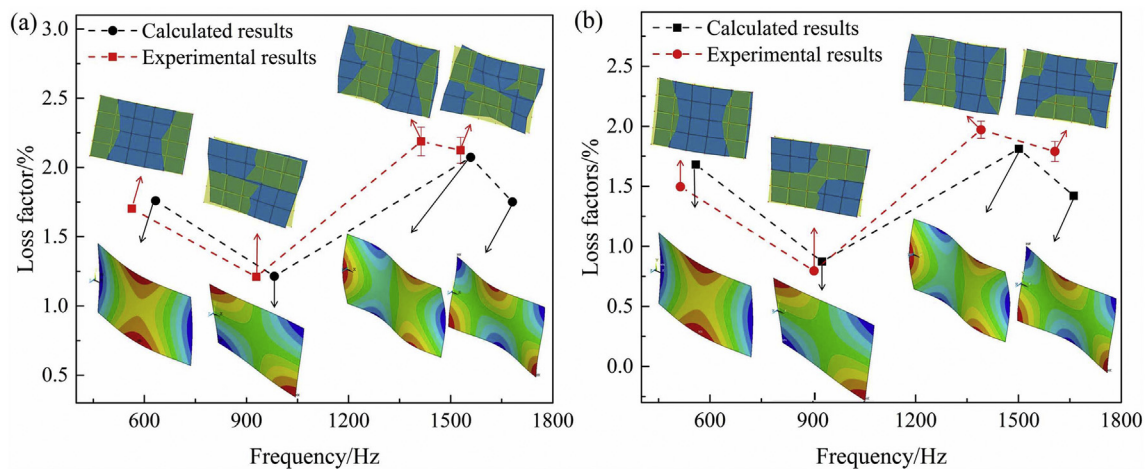


Fig. 8. First four modal parameters obtained by FEM and experiment: (a) CFRP/NH-1-1.83-64; (b) CFRP/NH-1-1.83-128.

## 5. Conclusions

Both the TSM and damping values of the Nomex honeycomb cores are greatly affected by the frequency and phenolic resin thickness. The TSM of the honeycomb core with thicker phenolic resin is more sensitive to the frequency. In addition, the sensitivity of TSM to the volume density only depends on the type of phenolic resin in theory, which is higher than the sensitivity of the damping values to the volume density. Therefore, compared with the damping properties, enhancing its mechanical properties (TSM) is relatively easier to be achieved by controlling the phenolic resin thickness. For the damping values,  $\eta_{LT}$  is about 7% higher than  $\eta_{WT}$  at relatively high frequency and their deviation is very small at low frequency, which implies that the honeycomb core with the maximum TSM and relatively large damping values in the LT direction might be used as candidate material in practical sandwich beam structures.

One-step forming process for the FRP/honeycomb sandwich structures with thin skins always results in the mechanical loss of the skins, which will further lead to overestimated damping values at the low frequency. This work might be helpful to manufacture or select the proper honeycomb materials for designers, especially when the service environment such as frequency is considered.

## Acknowledgements

This work was supported by the Special Research Foundation of China Civil Aircraft under Grant No. MJ-2015-H-G-103 and the Fundamental Research Funds of Shandong University under Grant No. 2016JC012.

## Appendix A. Supplementary data

Supplementary data related to this article can be found at <https://doi.org/10.1016/j.compositesb.2018.08.126>.

## References

- Giglio M, Manes A, Gilioli A. Investigations on sandwich core properties through an experimental–numerical approach. *Compos B Eng* 2012;43(2):361–74.
- Maheri MR, Adams RD, Hugon J. Vibration damping in sandwich panels. *J Mater Sci* 2008;43(20):6604–18.
- Rébillat M, Boutillon X. Measurement of relevant elastic and damping material properties in sandwich thick plates. *J Sound Vib* 2011;330(25):6098–121.
- Liu QL, Zhao Y. Effect of soft honeycomb core on flexural vibration of sandwich panel using low order and high order shear deformation models. *J Sandw Struct Mater* 2007;9(1):95–108.
- James S, Jonghwan S. Core material effect on wave number and vibrational damping characteristics in carbon fiber sandwich composites. *Compos Sci Technol* 2012;72(13):1493–9.
- Wang RS, Wang J. Modeling of honeycombs with laminated composite cell walls. *Compos Struct* 2018;184:191–7.
- Roy R, Park SJ, Kwon JH, Choi JH. Characterization of Nomex honeycomb core constituent material mechanical properties. *Compos Struct* 2014;117:255–66.
- Ralf Seemann, Krause Dieter. Numerical modelling of Nomex honeycomb sandwich cores at meso-scale level. *Compos Struct* 2017;159:702–18.
- Saito T, Parbery RD, Okuno S, Kawano S. Parameter identification for aluminum honeycomb sandwich panels based on orthotropic Timoshenko beam theory. *J Sound Vib* 1997;208(2):271–87.
- Jiang D, Zhang DH, Fei QG, Wu SQ. An approach on identification of equivalent properties of honeycomb core using experimental modal data. *Finite Elem Anal Des* 2014;90:84–92.
- Yang JS, Xiong J, Ma L, Feng LN, Wang SY, Wu LZ. Modal response of all-composite corrugated sandwich cylindrical shells. *Compos Sci Technol* 2015;115:9–20.
- Arun Kumar MP, Jagadeesh M, Pitchaimani J, Gangadharan KV, Lenin Babu MC. Sound radiation and transmission loss characteristics of a honeycomb sandwich panel with composite facings: effect of inherent material damping. *J Sound Vib* 2016;383:221–32.
- Adams RD, Maheri MR. The dynamic shear properties of structural honeycomb materials. *Compos Sci Technol* 1993;47(1):15–23.
- Petrone G, Rao S, Rosa S De, Mace BR, Franco F, Bhattacharyya D. Initial experimental investigations on natural fibre reinforced honeycomb core panels. *Compos B Eng* 2013;55:400–6.
- Petrone G, D'Alessandro V, Franco V, Rosa S De. Damping evaluation on eco-friendly sandwich panels through reverberation time (RT60) measurements. *J Vib Contr* 2014;21(16):3328–38.
- Nagasankar P, Balasivanandha Prabu S, Velmurugan R. Role of different fiber orientations and thicknesses of the skins and the core on the transverse shear damping of polypropylene honeycomb sandwich structures. *Mech Mater* 2015;91:252–61.
- Maheri MR, Adams RD. Steady-state flexural vibration damping of honeycomb sandwich beams. *Compos Sci Technol* 1994;52(3):333–47.
- Rueppel M, Rion J, Dransfeld C, Fischer C, Masania K. Damping of carbon fibre and flax fibre angle-ply composite laminates. *Compos Sci Technol* 2017;146:1–9.
- ASTM E756-05. Standard test method for measuring vibration-damping properties of materials. 2017.
- Cortés F, Elejabarrieta MJ. Viscoelastic materials characterisation using the seismic response. *Mater Des* 2007;28(7):2054–62.
- Blevins RD. Formulas for natural frequency and mode shape/reprinted. Krieger Pub. Co.; 2001. p. 106.
- Shahdin A, Mezeix L, Bouvet C, Morlier J, Gourinat Y. Fabrication and mechanical testing of glass fiber entangled sandwich beams: a comparison with honeycomb and foam sandwich beams. *Compos Struct* 2009;90(4):404–12.
- ASTM 393-00. Standard test method for flexural properties of sandwich constructions. 2000.
- Lin DX, Ni RG, Adams RD. Prediction and measurement of the vibrational damping parameters of carbon and glass fibre-reinforced plastics plates. *J Compos Mater* 1984;18(2):132–52.
- Bitzer T. Honeycomb technology: materials, design, manufacturing, applications and testing. Chapman & Hali; 1997. p. 215.
- Assarar M, El Mahi A, Berthelot JM. Evaluation of the dynamic properties of PVC foams under flexural vibrations. *Compos Struct* 2012;94(6):1919–31.
- Wang SQ, Wei C, Liu HX, Gong YY, Yang DJ, Yang P, Liu TX. Studies on mechanical properties and morphology of sisal pulp reinforced phenolic composites. *Adv Polym Technol* 2015;35(4):353–60.
- Wesolowski M, Barkanov E. Air damping influence on dynamic parameters of laminated composite plates. *Measurement* 2016;85:239–48.